

## PDF hosted at the Radboud Repository of the Radboud University Nijmegen

The following full text is a publisher's version.

For additional information about this publication click this link.

<http://hdl.handle.net/2066/35468>

Please be advised that this information was generated on 2017-12-06 and may be subject to change.

Rhodium-Mediated Stereoselective Polymerization of  
“Carbenes”

Dennis G. H. Hetterscheid,<sup>†</sup> Coen Hendriksen,<sup>†</sup> Wojciech I. Dzik,<sup>†</sup> Jan M. M. Smits,<sup>†</sup>  
Ernst R. H. van Eck,<sup>†</sup> Alan E. Rowan,<sup>†</sup> Vincenzo Busico,<sup>‡</sup> Michele Vacatello,<sup>‡</sup>  
Valeria Van Axel Castelli,<sup>‡</sup> Annalaura Segre,<sup>§</sup> Erica Jellema,<sup>||</sup>  
Tom G. Bloembergen,<sup>||</sup> and Bas de Bruin<sup>\*||</sup>

Contribution from the Institute for Molecules and Materials (IMM), Radboud University Nijmegen, Toernooiveld 1, 6525 ED Nijmegen, The Netherlands, Dipartimento di Chimica, Università di Napoli “Federico II”, Via Cintia, 80126 Naples, Italy, Istituto di Metodologie Chimiche, CNR, 00016 Montelibretti, Italy, and Department of Homogeneous Catalysis, Van ‘t Hoff Institute for Molecular Sciences (HIMS), University of Amsterdam, Nieuwe Achtergracht 166, 1018 WV, Amsterdam, The Netherlands

Received January 3, 2006; E-mail: bdebruin@science.uva.nl

**Abstract:** Unprecedented rhodium-catalyzed stereoselective polymerization of “carbenes” from ethyl diazoacetate (EDA) to give high molecular mass poly(ethyl 2-ylidene-acetate) is described. The mononuclear, neutral [(N,O-ligand)M](cod) (M = Rh, Ir) catalytic precursors for this reaction are characterized by (among others) single-crystal X-ray diffraction. These species mediate formation of a new type of polymers from EDA: carbon-chain polymers functionalized with a polar substituent at each carbon of the polymer backbone. The polymers are obtained as white powders with surprisingly sharp NMR resonances. Solution and solid state NMR data for these new polymers reveal a highly stereoregular polymer, with a high degree of crystallinity. The polymer is likely syndiotactic. Material properties are very different from those of atactic poly(diethyl fumarate) polymer obtained by radical polymerization of diethyl fumarate. Other diazoacetates are also polymerized. Further studies are underway to reveal possible applications of these new materials.

## Introduction

The thermal decomposition of diazomethane (reported around 1900) is the first known route to polymethylene.<sup>1</sup> Neither this explosive process, however, nor the milder catalytic versions<sup>2</sup> ever found large scale practical applications,<sup>3</sup> and it was more than half a century later that transition metal mediated ethene polymerization gave easy access to linear polyethylene.<sup>4,5</sup>

Unlike the inherently unstable diazoalkanes, diazocarbonyl compounds such as diazoacetates (N<sub>2</sub>CHCO<sub>2</sub>R) are reasonably stable, safe (even in large scale/industrial synthesis),<sup>6</sup> easy to prepare, and extensively used as carbene precursors in organic

synthesis. The most frequently observed reactions include carbene dimerization to form olefins, carbene transfer to olefins in cyclopropanation reactions, and carbene insertion into O–H, N–H, and C–H bonds. The reactions are often mediated by transition metals such as platinum, copper, rhodium acetates, and ruthenium catalysts, which have been reported to give efficient and, in many cases, stereoselective conversion of the carbenoid to more or less sophisticated products.<sup>7</sup> In this framework, though, only three reports describe the polymerization (oligomerization) of  $\alpha$ -carbonyl stabilized “carbenes” from diazocarbonyl compounds. This concerns Cu- and Pd-mediated formation of low molecular mass polymers (oligomers) from alkyl diazoacetates and related diazocarbonyls (number average degree of polymerization up to ca. 100).<sup>8,9</sup> These materials are notable because they carry a polar functionality

<sup>†</sup> Radboud University Nijmegen.

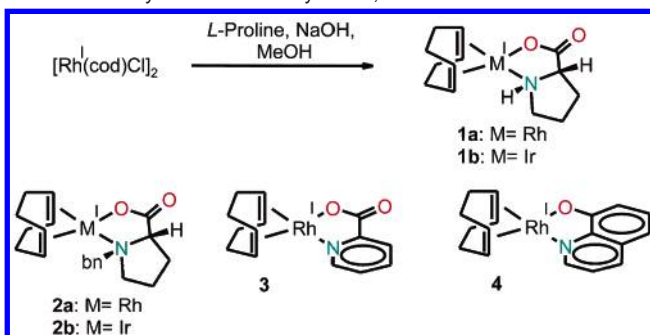
<sup>‡</sup> Università di Napoli “Federico II”.

<sup>§</sup> Istituto di Metodologie Chimiche.

<sup>||</sup> University of Amsterdam.

- (1) (a) von Pechmann, H. *Ber. Dtsch. Chem. Ges.* **1898**, *31*, 2643. (b) Bamberger, E.; Tchirner *Ber. Dtsch. Chem. Ges.* **1900**, *33*, 956.
- (2) (a) Feltzin, J.; Restaino, A. J.; Mesrobian, R. B. *J. Am. Chem. Soc.* **1955**, *77*, 206–210. (b) Bahwn, C. E. H.; Ledwith, A.; Matthies, P. *J. Pol. Sci.* **1959**, *34*, 93–108. (c) Cowel, G. W.; Ledwith, A. *Q. Rev. Chem. Soc.* **1970**, *24* (1), 119–167 and references therein.
- (3) For recent studies on polymethylene synthesis, see the following. (a) Via decomposition of diazomethane on TM surfaces: Bai, D.; Jennings, G. K. *J. Am. Chem. Soc.* **2005**, *127*, 3048. (b) Via boron-catalyzed polymerization of sulfoxonium ylides: Busch, B. B.; Paz, M. M.; Shea, K. J.; Staiger, C. L.; Stoddard, J. M.; Walker, J. R.; Zhou, X.-Z.; Zhu, H. *J. Am. Chem. Soc.* **2002**, *124*, 3636–3646 and references therein.
- (4) Ziegler–Natta catalyst: (a) Ziegler, K.; Breil, H.; Martin, H.; Holzkamp, R. German Patent 973726, 1953. (b) Natta, G.; Pino, P.; Mazzanti, G. U.S. Patent 3715344, 1954. (c) Natta, G. *J. Polym. Sci.* **1955**, *16*, 143–154.
- (5) Phillips catalyst: Hogan, J. P.; Banks, R. L. U.S. Patent 2,825,721, 1985. (b) McDaniel, M. P. *Adv. Catal.* **1995**, *33*, 47–98.

- (6) (a) Clarck, J. D.; Shah, A. S.; Peterson, J. C. *Thermochim. Acta* **2002**, *392–392*, 177–186. (b) Clarck, J. D.; Shah, A. S.; Peterson, J. C.; Patelis, L.; Kersten, R. J. A.; Heemskerck, A. H. *Thermochim. Acta* **2002**, *386*, 73–79. (c) Clarck, J. D.; Shah, A. S.; Peterson, J. C.; Patelis, L.; Kersten, R. J. A.; Heemskerck, A. H.; Grogan, M.; Camden, S. *Thermochim. Acta* **2002**, *386*, 65–72. (d) Clarck, J. D.; Heise, J. D.; Shah, A. S.; Peterson, J. C.; Chou, S. K.; Levine, J.; Karakas, A. M.; Ma, Y.; Ng, K.-Y.; Patelis, L.; Springer, J. R.; Stano, D. R.; Wettach, R. H.; Dutra, G. A. *Org. Process Res. Dev.* **2004**, *8*, 176–185.
- (7) (a) Merlic, C. A.; Zechman, A. L. *Synthesis* **2003**, 1137. (b) Ye, T.; McKervey, A. *Chem. Rev.* **1994**, *94*, 1092. (c) Maas, G. *Chem. Soc. Rev.* **2004**, *33*, 183.
- (8) Liu, L.; Song, Y.; Li, H. *Polym. Int.* **2002**, *51*, 1047.
- (9) (a) Ihara, E.; Haida, N.; Iio, M.; Inoue, K. *Macromolecules* **2003**, *36*, 36. (b) Ihara, E.; Fujioka, M.; Haida, N.; Itoh, T.; Inoue, K. *Macromolecules* **2005**, *38*, 2101.

**Scheme 1.** Synthesis of Catalysts **1a,b** and the Structure of **2–4**

(amenable to further transformations) at each main chain C atom—a structure which is not accessible via Ziegler–Natta catalysis<sup>4</sup> and had only been obtained so far from dialkyl maleates or fumarates by free radical processes,<sup>10</sup> with no control on the resultant polymer stereochemistry. As such, carbene polymerization seems an attractive route to prepare functionalized polymers. However, stabilized diazocarbonyl compounds are notoriously more difficult to polymerize than their nonsubstituted diazoalkyl analogues. Presently, there are no catalysts known that produce high molecular mass or stereoregular polymethylenes with functional side groups. As a consequence of their low molecular mass, materials obtained thus far (i.e. in the above Cu and Pd mediated reactions) are rather unattractive viscous oils with very broad NMR resonances.

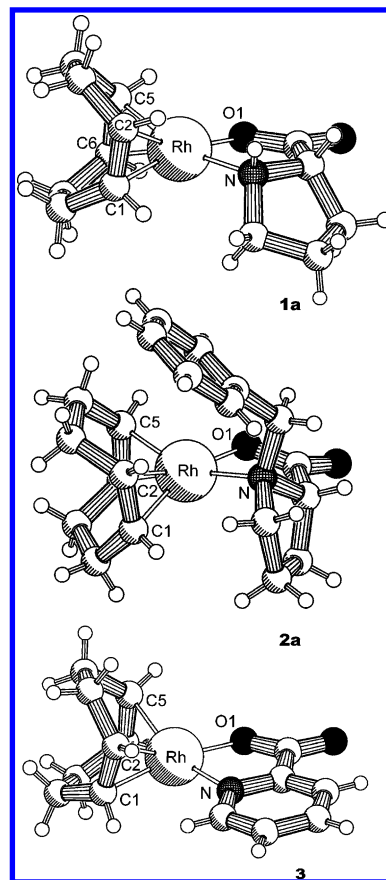
In this article, we report the stereoselective polymerization of carbenes generated from alkyl diazoacetates to high molecular mass poly(alkyl 2-ylideneacetate)s (PEA;  $M_w$  up to 190 kDa as white solids with sharp NMR resonances) in the presence of rhodium-based catalysts.

## Results and Discussion

**Synthesis and Characterization of the Catalysts.** The  $[M^I(L\text{-prolinate})(cod)]$  complexes **1a** ( $M = Rh$ ) and **1b** ( $M = Ir$ ) ( $cod = Z,Z\text{-}1,5\text{-cyclooctadiene}$ ) were prepared by reaction of the  $[(cod)M^I(Cl)]_2$  precursors with in situ deprotonated L-proline in methanol at room temperature (Scheme 1). The benzyl analogues  $[M^I(N\text{-benzyl-L-prolinate})(cod)]$  (**2a**,  $M = Rh$ ; **2b**,  $M = Ir$ ) and the nonchiral picolinate and quinolate Rh analogues **3** and **4** were prepared via similar routes. The structures of **1–3** were determined by single-crystal X-ray diffraction (Figure 1; Table 1). The reported structure of **4** is very similar.<sup>11</sup>

Complexes **1–4** all adopt a square-planar geometry. The picolinate ligand in **3** is planar and causes little steric hindrance to the two trans vacant sites of the Rh center. The aliphatic proline ring of **1a** on the other hand is bent, thus shielding one of the two vacant sites somewhat from its environment. This effect is more pronounced for the *N*-benzyl-L-prolinate analogue **2a**. The Ir species **2b** is isostructural to its Rh analogue **2a**. The M–ligand bond lengths of **1–4** are quite comparable. The variations in the M–N bond lengths in the order  $N_{Py} < NHR_2 < NR_3$  are as expected for  $sp^2$  and secondary and tertiary  $sp^3$  hybridized nitrogen atoms.

**Polymerization of Carbenes from Diazoacetates.** Doyle-type dinuclear tetracarboxylate-bridged  $Rh^{II}\text{--}Rh^{II}$  species have been extensively studied as catalysts for a variety of carbene

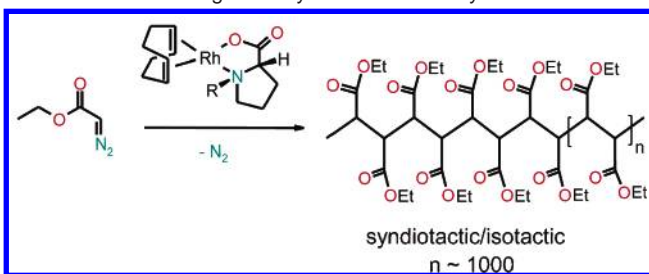
**Figure 1.** X-ray structures of **1a**, **2a**, and **3**.**Table 1.** Selected Bond Lengths (Å) and Angles (deg) Observed for Complexes **1–3**

param	1a (M = Rh)	2a (M = Rh)	2b (M = Ir)	3 (M = Rh)
M–O1	2.042(2)	2.0593(11)	2.0548(15)	2.0597(13)
M–N	2.109(2)	2.1558(14)	2.152(2)	2.0857(16)
M–C1	2.095(3)	2.0986(15)	2.092(2)	2.1028(19)
M–C2	2.088(3)	2.1155(15)	2.108(2)	2.084(2)
M–C5	2.124(3)	2.1049(17)	2.099(2)	2.1370(19)
M–C6	2.115(3)	2.1432(17)	2.127(3)	2.127(2)
O1–M–N	81.88(8)	79.61(5)	79.40(7)	80.00(6)
O1–M–C1	163.61(18)	155.49(6)	155.74(8)	164.13(7)
N–M–C1	96.58(12)	98.84(7)	100.00(9)	100.45(7)

transfer reactions using diazoacetates as carbene precursors.<sup>12</sup> It has always been assumed that the  $Rh^{II}\text{--}Rh^{II}$  bond of these catalysts stays intact during catalysis, but no synergistic effects have so far been proven. Whereas these species have a formal  $Rh^{II}$  oxidation state, they can also be considered as  $Rh^I\text{--}Rh^{III}$  species. Therefore, it is quite possible that mononuclear  $Rh^I$ ,  $Rh^{III}$ , and/or  $Rh^{II}$  oxidation state species are the actual catalytically active species. In fact, Bergman, Tilley, and co-workers described in a recent paper that mononuclear  $Rh^{II}$  species can indeed function as active catalysts for carbene transfer reactions.<sup>13</sup> This work inspired us to investigate carbene transfer reactions mediated by mononuclear  $Rh^I$  species.

Initially we aimed at catalytic cyclopropanation of olefins, using ethyl diazoacetate (EDA) as a carbene precursor and the

(10) Toyoda, N.; Yoshida, M.; Otsu, T. *Polym. J.* **1983**, *15*, 255.(11) Leipoldt, J. G.; Grobler, E. C. *Inorg. Chim. Acta* **1983**, *72*, 17.(12) See for example: Davies, H. M. L.; Beckwith, R. E. J. *Chem. Rev.* **2003**, *103*, 2861 and references therein.(13) Krumper, J. R.; Gerisch, M.; Suh, J. M.; Bergman, R. G.; Tilley, T. D. J. *Org. Chem.* **2003**, *68*, 9705.

**Scheme 2.** Stereoregular Polymerization of Ethyl Diazoacetate**Table 2.** Polymerization of EDA with Catalysts **1–4**<sup>a</sup>

entry	catalyst	$T_r$ , °C	solvent	reacn time	yield, % <sup>b</sup>	$M_n$ , kDa	$M_w/M_n$
1	<b>1a</b>	-20	CHCl <sub>3</sub>	7 days	50	190	3.3
2	<b>1a</b>	0	CHCl <sub>3</sub>	3 days	35	169	3.0
3	<b>1a</b>	20	CHCl <sub>3</sub>	14 h	45	133	2.4
4	<b>1a</b>	20	CHCl <sub>3</sub>	30 min	5	49	2.0
5	<b>1a</b>	40	CHCl <sub>3</sub>	14 h	30	100	2.2
6	<b>1a</b>	20	MeCN	14 h	10	82	2.2
7	<b>1a</b>	20	CH <sub>2</sub> Cl <sub>2</sub>	14 h	40	143	2.5
8	<b>1a</b>	20	THF	14 h	35	130	2.4
9	<b>1a</b>	20	C <sub>7</sub> H <sub>8</sub>	14 h	25	120	2.7
10	<b>2a</b>	20	CHCl <sub>3</sub>	14 h	25	154	2.7
11	<b>1b</b> (M = Ir)	20	CHCl <sub>3</sub>	14 h	0		
12	<b>2b</b> (M = Ir)	20	CHCl <sub>3</sub>	14 h	4	12	1.6
13	<b>3</b>	20	CHCl <sub>3</sub>	14 h	15	132	2.5
14	<b>4</b>	20	CHCl <sub>3</sub>	14 h	15	147	2.9

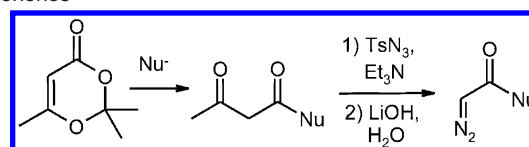
<sup>a</sup> Conditions: 0.037 mmol of catalysts; 1.84 mmol of EDA, 6 mL of solvent. <sup>b</sup> After precipitation with MeOH.

chiral Rh<sup>I</sup> complex **1a** as a catalytic precursor. Cyclopropanation of styrene is indeed mediated by **1a** but only in low yields (~12%) with hardly any cis/trans specificity (53:47) and without any enantioselectivity. As expected, **1a** also catalyzes carbene dimerization yielding diethyl maleate and diethyl fumarate in a 58:42 ratio. However, while **1a** mediates full conversion of EDA, this yields at most 40% diethyl maleate and diethyl fumarate according to NMR. The remaining material (~60%) proved to be the new poly(ethyl 2-ylideneacetate) polymer (PEA, Scheme 2). Formation of PEA was further investigated using the catalysts **1–4**.

Treating EDA with a catalytic amount of **1–4** (2 mol %) gave PEA in isolated yields between 10% and 50% depending on the reaction conditions (Table 2). The polymer was separated from the reaction mixture by quenching with methanol, yielding PEA as a white powder. The highest yields in polymer were observed with **1a** in chloroform or dichloromethane. In other solvents (e.g., THF, acetonitrile, or toluene) yields were lower, possibly due to partial catalyst precipitation.

Molecular masses of the new PEA polymers were determined from size exclusion chromatography (SEC) measurements calibrated with matrix-assisted laser light scattering (MALLS). At 20 °C, with all four rhodium-based catalysts high molecular mass polymers were obtained ( $M_w$  typically in the range 120–155 kDa) within 14 h. Not unexpectedly, shortening the reaction time leads to formation of lower weight polymers in lower yields (Table 2, entry 4). Decreasing the reaction temperature and increasing the reaction time leads to an increase of the polymer molecular mass ( $M_w$  up to 190 kDa for polymerization with **1a** in chloroform at -20 °C).

The polydispersities of the polymers obtained with the Rh catalysts are all slightly higher than 2.0. The polymerization experiments were run with full conversion of EDA, which

**Scheme 3.** Preparation of Diazocarbonyl Compounds from Dioxenones

contributes to somewhat broader weight distributions (Table 2, entries 3 and 4). Therefore, we consider the obtained polydispersities to be in agreement with a nonliving polymerization process at a single center active species.

Quite remarkably, **1b** (the iridium analogue of **1a**) does not produce any PEA polymer from EDA. Instead, **1b** catalyzes quantitative carbene dimerization to yield a mixture of diethyl fumarate and diethyl maleate (in a ratio of 1:9). Iridium complex **2b** on the other hand, containing a weaker coordinating benzyl-functionalized N-donor, does produce PEA in low yields (4%). Both the molecular weight ( $M_w = 12$  kDa) and the polydispersity ( $M_w/M_n = 1.6$ ) of the polymer obtained with **2b** are much lower than those of the polymers obtained with the Rh species.

A variety of diazocarbonyl “monomers” are readily obtained via cheap and easy routes. Addition of nucleophiles to dioxenones, followed by diazo transfer to the resulting  $\beta$ -keto esters and base-assisted elimination of acetic acid, provides a convenient route to such species (Scheme 3).<sup>7,14</sup> Preliminary results reveal that treatment of thus obtained crude 3-butenyldiazoacetate (Nu = -OCH<sub>2</sub>CH<sub>2</sub>CH=CH<sub>2</sub>) and 3-butyndiazoacetate (Nu = -OCH<sub>2</sub>CH<sub>2</sub>C≡CH) with **1a** yields the corresponding polymers, albeit in low yields (2–8%). Copolymers from 3-butenyldiazoacetate and EDA (1:10) are obtained in higher yields (32%). Polymerization of *n*-butyldiazoacetate (Nu = -OBu) gives a yield of ~20%. Clearly, the scope of the catalytic process introduced herein is not limited to EDA, and we are currently investigating other diazocarbonyl compounds as carbene precursors in Rh-mediated polymerization reactions.

**Characterization of Stereoregular PEA.** Quite surprisingly, the new high molecular weight PEA polymers obtained with catalysts **1–4** reveal sharp resonances in solution <sup>1</sup>H and <sup>13</sup>C NMR spectra indicative for stereoregular polymers. The low molecular weight ( $M_w \sim 1.2$  kDa) PEA polymers (oligomers) obtained with Pd-based catalysts reported by Ihara and co-workers are viscous oils which show very broad NMR resonances.<sup>9a</sup> Apart from the possibility that these polymers are atactic, the broadening of the NMR signals of these low molecular weight polymers could also be caused by chain-end effects. For none of the PEA samples obtained with the Rh and Ir catalysts **1–4** we were able to detect polymer chain-end signals or indirect chain-end effects with NMR. To investigate tacticity effects, we prepared atactic PEA by radical polymerization (initiated by AIBN) of diethyl fumarate.<sup>9a,10</sup> These atactic PEA samples have a larger molecular weight ( $M_w = 6.1$  kDa) but still reveal very broad NMR resonances. NMR spectra of the new stereoregular PEA polymers obtained with catalysts **1–4** are clearly different from those of atactic PEA (Figure 2).

Even at 600 MHz for <sup>1</sup>H NMR and 150 MHz for <sup>13</sup>C NMR, the main chain methine signal of stereoregular PEA appears as a highly symmetrical singlet, with a half-height width of 11 and 20 Hz, respectively. A weak shoulder at higher frequency

(14) (a) Clemens, R. J.; Hyatt, J. A. *J. Org. Chem.* **1985**, *50*, 2431. (b) Li, G.-Y.; Che, C.-M. *Org. Lett.* **2004**, *6*, 1621.

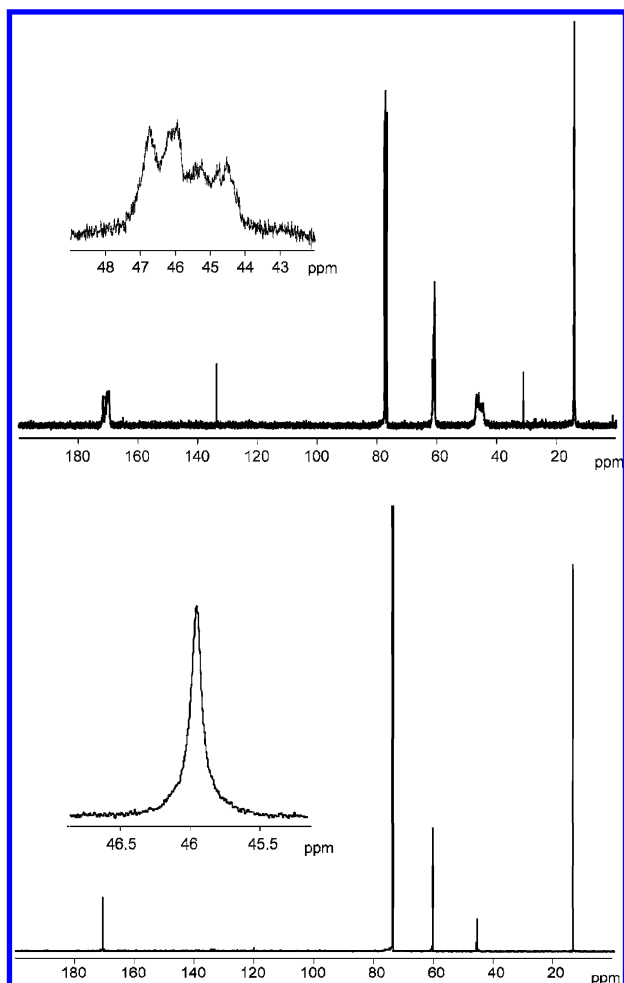


**Figure 2.**  $^{13}\text{C}$  NMR spectra of atactic PEA obtained with radical polymerization of diethyl fumarate (top) and stereoregular PEA obtained by Rh-mediated polymerization of EDA (catalyst **1a**).

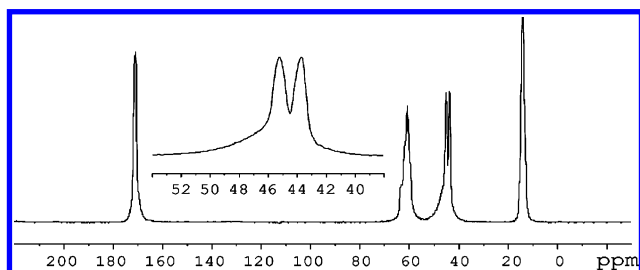


**Figure 3.**  $^{13}\text{C}$  CP/MAS NMR spectrum of a typical PEA sample.

of the  $^1\text{H}$  NMR signal is possibly traceable to stereo defects (in all cases well below 10%, as estimated by peak deconvolution).

Solid-state NMR is consistent with the above conclusion and provides more information. In the CP/MAS NMR spectrum<sup>15</sup> (Figure 3), the methine signal reveals two sharp resonances ( $\delta = 43.73$  and  $45.30$  ppm) in an approximate 1:1 ratio, partly overlapped by a weaker and broader peak at higher frequency ( $\delta = 47.8$  ppm). The former can be attributed to a crystalline phase, while the latter represents an amorphous fraction. Fourier transformation with a resolution enhancing window function revealed a similar splitting for the carbonyl peak (1:1 sharp doublet at  $\delta = 171.0$  and  $171.8$  ppm) and more complicated

fine structures for the methylene ( $\delta = 59.6$ – $63.7$  ppm) and methyl ( $\delta = 12.8$ – $14.6$  ppm) peaks (Supporting Information, Figure S6 and S7).

By deconvolution of the methine resonance in a quantitative single pulse  $^{13}\text{C}$  MAS NMR spectrum (recycle time, 60 s), the relative abundance of the crystalline phase was estimated to be slightly above 70%. In a single pulse  $^{13}\text{C}$  MAS NMR spectrum run with very short recycle time (1 s), so as to minimize the contribution of more rigid, ordered structures, which generally tend to have a longer  $T_1$  relaxation time,<sup>16</sup> the methylene and methyl resonances turned out to be clearly stronger than the methine and carbonyl ones, which suggests some conformational disorder of the ethyl residue even in the crystalline domains. Powder X-ray diffraction spectra of stereoregular PEA reveal strong but relatively broad peaks (Supporting Information, Figure S9). This seems in good agreement with a high degree of crystallinity but with substantial disorder of the ethyl residues.

Stereoregular PEA can in principle be isotactic or syndiotactic. Preliminary molecular mechanics (MM2) calculations on model compounds indicated that low-energy conformations with a two-backbone-bond conformational repeat are found for both polymers in the TG (trans-gauche) and GT domains; this is consistent with a shift to lower frequency of the methine peak for the ordered phase relative to the disordered one in the CP/MAS NMR spectrum. The H–C–C=O torsions are all close to anti (anti  $\sim 160^\circ$ ) in the isotactic polymer, whereas their sequence in the syndiotactic polymer is ...syn, syn, anti, anti, syn, syn... (syn  $\sim 30^\circ$ , anti  $\sim 170^\circ$ ), with the syn, anti or anti, syn arrangements flanking the main chain T bonds. The SCF-MO calculated NMR spectra are compatible with the experimental one for both structures; therefore additional information is needed for a definitive assignment of the configuration. We recently prepared carbonyl  $^{13}\text{C}$ -labeled samples of the new stereoregular PEA polymers, and we are currently investigating their configuration by 2-dimensional carbon–carbon correlation experiments (DOQSY).<sup>17</sup> Analyzing the results of these experiments is not straightforward and requires elaborate data-fitting.<sup>18</sup> These results will be published in a subsequent paper.

**(a) Thermal Analysis.** Stereoregular PEA as obtained by precipitation from the reaction mixture with MeOH is largely amorphous. However, slow evaporation of the solvent from a solution of stereoregular PEA in chloroform results in a “crystallized” brittle film of the polymer. These “amorphous” and crystallized samples of stereoregular PEA have different properties.

Thermogravimetric measurements (TGA) reveal that both the amorphous and crystallized PEA samples decompose above  $300^\circ\text{C}$ , but DSC data for these samples at lower temperatures are clearly different from each other. The amorphous samples showed a reversible first-order phase transition at  $100^\circ\text{C}/75^\circ\text{C}$  on heating/cooling (Supporting Information, Figure S11). In the first heating/cooling cycle these transitions are very weak but become stronger ( $\Delta h = 21 \text{ J g}^{-1}$ ) in a second cycle after annealing the polymer for a few seconds at  $240^\circ\text{C}$ .

Samples which were first crystallized from  $\text{CHCl}_3$  reveal quite pronounced ( $\Delta h = 24 \text{ J/g}$ ) and sharp DSC transitions from the beginning, without the need to anneal the polymer (see Figure

(15) Bovey, F. A.; Mirau, P. A. In *NMR of Polymers*; Academic Press: San Diego, CA, 1969; Chapter 4.

(16) Fyfe, C. A.; Lyerla, J. R.; Volksen, W.; Yannoni, C. S. *Macromolecules* **1979**, *12*, 757–761.

(17) Schmidt-Rohr, K. *Macromolecules* **1996**, *29*, 3975–3981.

(18) Van Beek, J. D.; Meier, B. H. *J. Magn. Res.* **2006**, *178*, 106–120.

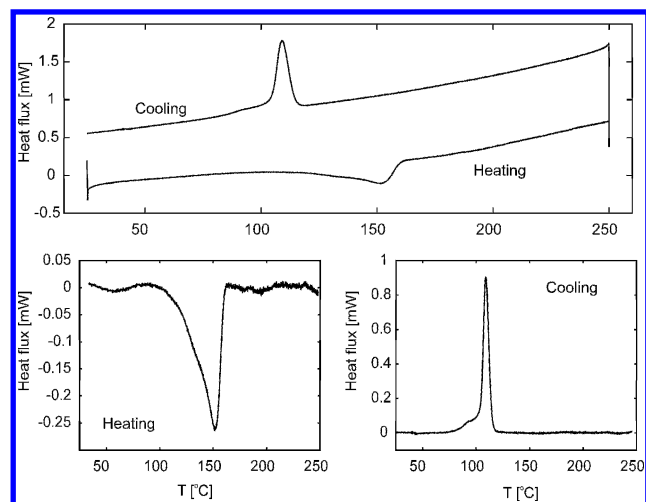


**Figure 4.** DSC 2nd heating and cooling curves of a “crystallized” sample of stereoregular PEA (entry 3, Table 2, after dissolution in chloroform and slow evaporation of the solvent).

4). The transitions of the crystallized samples also occur at higher temperatures (150 °C/110 °C) compared to those of the amorphous samples (100 °C/75 °C). Since the polymer is a flexible rubber above 155 °C, whereas it is hard and brittle below 70 °C, the transitions at 150 °C/110 °C for crystallized PEA and 100 °C/75 °C for amorphous PEA could be interpreted as the softening and glass-transition temperatures, in accord with reported glass–rubber transitions of atactic PEA (between 65 and 80 °C).<sup>10</sup> The fact that crystallized samples of stereoregular PEA reveal transitions at higher temperatures compared to the amorphous samples and the fact that these transitions appear as real peaks in the DSC could point to a substantial influence of the glass–rubber transitions by the crystalline domains of this material.<sup>19</sup> However, at this point we cannot exclude an alternative interpretation of the data, in which the DSC peaks correspond to crystalline–liquid crystalline transitions instead of glass–rubber transitions. We are currently investigating this possibility.

The reported softening (78–80 °C) and glass transition temperatures (65 °C) of atactic PEA (obtained by radical polymerization of diethyl maleate with AIBN)<sup>10</sup> are somewhat lower than the above transitions of our amorphous stereoregular PEA. For bulky polymers, containing only one repeating side group/two carbons of the polymer backbone, the highest glass transition temperatures are usually observed for the atactic and syndiotactic polymers.<sup>19,20</sup> For poly[methyl(methacrylate)] (PMMA)<sup>21,22</sup> for example, quite large differences in glass transition temperatures are reported for the atactic (~90 kDa,  $T_g = 105$  °C),<sup>22</sup> isotactic (30 kDa,  $T_g = 56$  °C),<sup>21b</sup> and syndiotactic (60 kDa,  $T_g = 140$  °C)<sup>21b</sup> polymers. Van der Waals forces between polymeric chains in amorphous domains are stronger for the less symmetrical atactic and syndiotactic polymers as compared to isotactic polymers. If one reasons in analogy (and assumes that the transitions belong to glass–rubber transitions), stereoregular PEA might be syndiotactic because

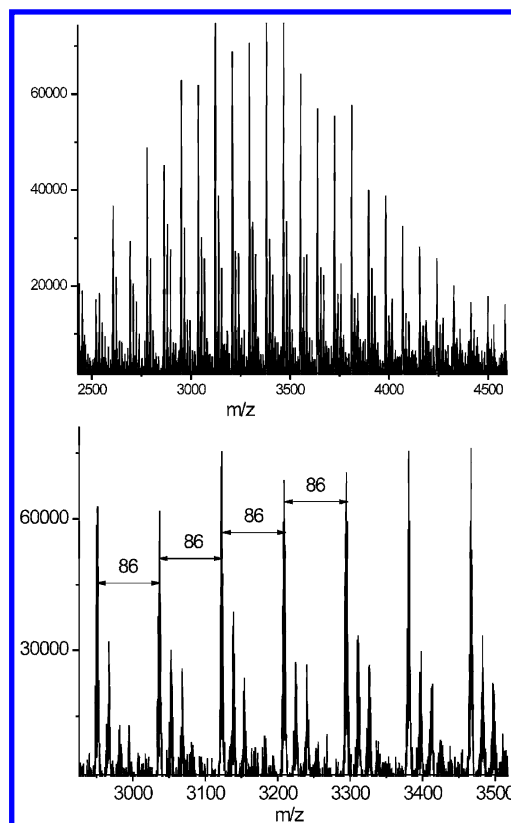


**Figure 5.** MALDI-TOF spectra (reflection mode) of PEA obtained with catalyst **2b** (Table 2, entry 12).

even the amorphous samples reveal transitions at higher temperatures than atactic PEA. However, since we have no reference material for glass–rubber transitions of atactic, isotactic, and syndiotactic carbon-chain polymers which are substituted at each carbon of the polymer backbone (nor information excluding the alternative interpretation of the transitions as crystalline–liquid crystalline transitions), these data are only an indication for the possible configuration of stereoregular PEA.

Under a polarization microscope, the crystallized PEA samples show birefringence. Above the softening temperature, also the amorphous PEA samples start to show birefringence but only after physical contact. We take the birefringence as a further indication for the semicrystalline behavior of stereoregular PEA (or perhaps thermotropic liquid-crystalline behavior in the rubber state).

**(b) MALDI-TOF.** The polymers prepared with Rh catalysts **1a**, **2a**, **3**, and **4** invariably give high molecular weight PEA polymers with rather broad molecular weight distributions ( $M_w/M_n = 2–3$ ; see Table 2). As expected, we were unable to measure any reliable MALDI-TOF mass spectra from these PEA samples. However, MALDI-TOF spectra of PEA prepared with Ir catalyst **2b** ( $M_w = 12$  kDa,  $M_w/M_n = 1.6$ ) were readily obtained, albeit only in the lower mass region of the polymer. As shown in Figure 5, PEA is clearly built from ethyl 2-ylideneacetate (:CHCOOEt) repeating units, resulting in a regular 86 Da spaced repeating pattern. Fragments with an equal number degree of polymerization ( $n$ ) give rise to three masses:  $(\text{CHCOOEt})_n + 25 + x \times 86$  Da (dominant signals),  $(\text{CHCOOEt})_n + 41 + x \times 86$  Da (weaker), and  $(\text{CHCOOEt})_n + 56 + x \times 86$  Da (least intense).

(19) Stevens, M. P. *Polymer Chemistry, An introduction*, 3rd ed.; Oxford University Press: New York, 1999.

(20) Burfield, D. R.; Doi, Y. *Macromolecules* **1983**, *16*, 702–704.

(21) (a) Collins, S.; Ward, D. G. *J. Am. Chem. Soc.* **1992**, *114*, 5460. (b) Bolig, A. D.; Chen, E. Y. X. *J. Am. Chem. Soc.* **2001**, *123*, 7943. (c) Deng, H.; Shiono, T.; Soga, K. *Macromolecules* **1995**, *28*, 3067. (d) Cui, C.; Shafir, A.; Reeder, C. L.; Arnold, J. *Organometallics* **2003**, *22*, 3357.

(22) Porter, C. E.; Blum, F. D. *Macromolecules* **2000**, *33*, 7016.

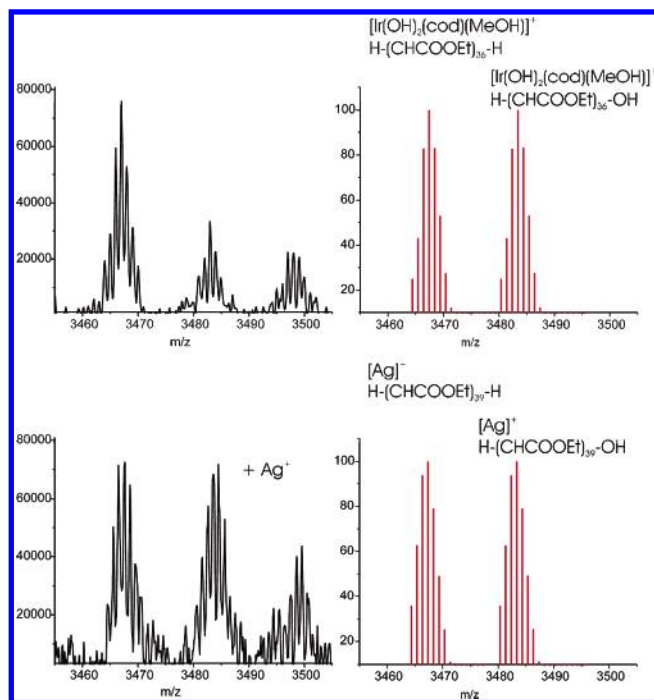
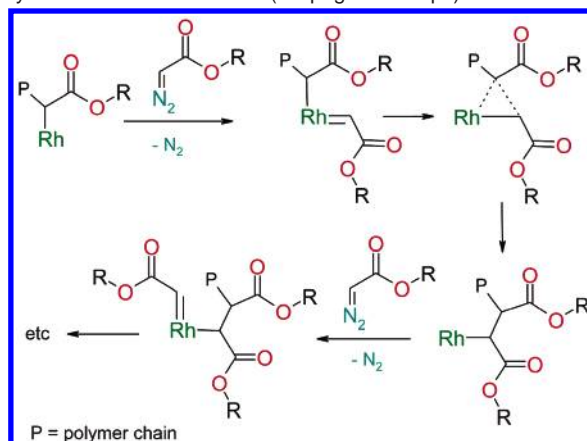


**Figure 6.** Experimental MALDI-TOF MS spectra of PEA (reflection mode) without (top, left) and with addition of  $\text{Ag}^+$  (bottom, left) as a cationization agent and calculated isotope distributions of H-PEA-H and H-PEA-OH chains with an Ir complex (top, right) and  $\text{Ag}^+$  (bottom, right) as charge carriers.

Although the masses of the more intense signals correspond with  $[\text{Na}]^+\{(\text{H}-\text{CHCOOEt})_n-\text{H}\}$  (e.g.  $m/z = 3467$  Da, with  $n = 36$ ) and  $[\text{Na}]^+\{(\text{H}-\text{CHCOOEt})_n-\text{OH}\}$  (e.g.  $m/z = 3483$  Da, with  $n = 36$ ), these interpretations do not explain their typical isotope distribution patterns. These patterns are suggestive for the presence of cationic iridium complexes as charge carriers (Figure 6). The signals could well belong to  $[\text{Ir}^{\text{III}}(\text{OH})_2(\text{cod})(\text{MeOH})]^+\{(\text{H}-\text{CHCOOEt})_n-\text{H}\}$  (e.g.  $m/z = 3467$  Da, with  $n = 36$ ) and  $[\text{Ir}^{\text{III}}(\text{OH})_2(\text{cod})(\text{MeOH})]^+\{(\text{H}-\text{CHCOOEt})_n-\text{OH}\}$  (e.g.  $m/z = 3483$  Da, with  $n = 36$ ), but with different Ir-bound ligands alternative interpretations are possible.<sup>23</sup> Addition of  $\text{K}^+$  salts does not influence the spectrum. Addition of  $\text{Ag}^+$  salts does not change the peak positions but does influence their relative intensities, leading to significantly increased intensities of the  $(\text{CHCOOEt})_n + 41 + x \times 86$  Da signals (e.g. 3483 Da). Also the isotopic distribution patterns appear to be different in the presence of  $\text{Ag}^+$ . The coincidentally unchanged masses with slightly different isotopic distribution patterns are suggestive for the presence of  $[\text{Ag}]^+\{(\text{H}-\text{CHCOOEt})_n-\text{H}\}$  and  $[\text{Ag}]^+\{(\text{H}-\text{CHCOOEt})_n-\text{OH}\}$ . Considering the increased intensity of the  $(\text{CHCOOEt})_n + 41 + x \times 86$  Da signals in the presence of  $\text{Ag}^+$ , it seems quite safe to conclude that H- $(\text{CHCOOEt})_n-\text{OH}$  chains are present in the polymer samples. The MS data are also suggestive for the copresence of H- $(\text{CHCOOEt})_n-\text{H}$  chains, although this picture

(23) Assuming the presence of iridium, the observed masses could (among others) correspond to the following:  $[\text{Ir}^{\text{III}}(\text{OH})_2(\text{cod})(\text{MeOH})]^+\{(\text{H}-\text{CHCOOEt})_n-\text{H}\}$  (3467 Da for  $n = 36$ );  $[\text{Ir}^{\text{III}}(\text{OH})_2(\text{cod})(\text{MeOH})]^+\{(\text{H}-\text{CHCOOEt})_n-\text{OH}\}$  (3483 Da for  $n = 36$ );  $[\text{Ir}^{\text{IV}}(\text{OH})(\text{cod})(\text{MeOH})_2]^+\{(\text{H}-\text{CHCOOEt})_n-\text{H}\}$  (3498 Da for  $n = 36$ );  $[\text{Ir}^{\text{III}}(\text{OH})_2(\text{H}_2\text{O})_3]^+\{(\text{H}-\text{CHCOOEt})_n-\text{H}\}$  (3467 Da for  $n = 37$ );  $[\text{Ir}^{\text{III}}(\text{OH})_2(\text{H}_2\text{O})_3]^+\{(\text{H}-\text{CHCOOEt})_n-\text{OH}\}$  (3483 Da for  $n = 37$ );  $[\text{Ir}^{\text{III}}(\text{OH})_2(\text{H}_2\text{O})_3(\text{HOME})]^+\{(\text{H}-\text{CHCOOEt})_n-\text{H}\}$  (3499 Da for  $n = 37$ );  $[\text{Ir}^{\text{III}}(\text{OH})_2(\text{MeOH})(\text{H}_2\text{O})_2]^+\{(\text{H}-\text{CHCOOEt})_n-\text{OH}\}$  (3497 Da for  $n = 36$ );  $[\text{Ir}^{\text{III}}(\text{OMe})_2(\text{MeOH})_4]^+\{(\text{H}-\text{CHCOOEt})_n-\text{H}\}$  (3483 Da for  $n = 36$ );  $[\text{Ir}^{\text{I}}(\text{cod})(\text{MeOH})(\text{OH})_2]^+\{(\text{H}-\text{CHCOOEt})_n-\text{OH}\}$  (3483 Da for  $n = 36$ ).

**Scheme 4.** Proposed Formation of PEA via Insertion Polymerization of "Carbenes" (Propagation Steps)



is somewhat blurred (no clear intensity change upon addition of  $\text{Ag}^+$  and overlapping signals of Ir-based alternatives).<sup>23</sup>

At this point we cannot entirely exclude the possibility of organometallic rhodium or iridium complexes being present as polymer chain ends. PEA samples obtained with catalyst **1a** reveal the presence of 0.09% Rh, which corresponds to approximately 1 equiv of Rh/polymer chain. Therefore, a final assignment of the polymer end groups (i.e. Rh/Ir based, only H-PEA-OH or a mixture of both H-PEA-OH and H-PEA-H) requires additional data from high-resolution MS spectra (requiring polymer samples with a lower polydispersity) and/or NMR characterization of lower molecular weight polymers.

**Mechanistic Considerations.** At this point we do not understand all details of the formation of PEA. We need a high catalyst loading of 2% to obtain complete conversion of EDA. Half of the starting material converts to diethyl maleate and diethyl fumarate. Since polymers consisting of about 1000 CHCOOEt repeating units are formed, only about 3% of the added catalytic precursor becomes really active as a polymerization catalyst. The exact nature of the active species is therefore unknown, and in part we necessarily rely on (educated) speculations in the mechanistic considerations below.

The nature of the catalyst has little influence on the obtained stereoregular PEA. The Rh-based catalytic precursors **1a**, **2a**, **3**, and **4** produce roughly the same molecular weight PEA with comparable polydispersities. Only the Ir-based precursor **2b** produces somewhat lower molecular weight PEA. There are no obvious differences in the properties between the obtained polymers (including NMR data), suggesting that identical or at least very similar active species are generated. This likely involves dissociation of the *N,O*-ligand from the metal under catalytic conditions. However, the precursors **1a**, **2a**, **3**, and **4** produce PEA in different yields, thus suggesting that the *N,O*-ligands do have an influence on the kinetics of initiation. This might, for example, involve formation of a reactive metal-alkyl by attack of a nitrogen donor (as in the Pd-based systems of Ihara et al.)<sup>9</sup> or oxygen donor of the *N,O*-ligand to a metal-bound carbene. The MALDI-TOF spectra further suggest the presence of -H and -OH end groups. Chain growth might thus start from M-OH and/or M-H species, while termination might involve reductive elimination of M(H)(C<sub>chain</sub>) fragments, protonation of M-C<sub>chain</sub> fragments, and/or oxidation (by e.g. O<sub>2</sub>).

Formation of a rhodium-bound carbene is commonly believed to be a key step in rhodium-catalyzed carbene transfer reactions

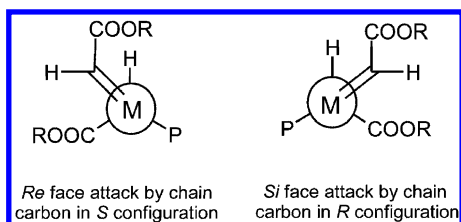


**Figure 7.** “Chain-end control” in the stereoselective polymerization of “carbenes” from EDA leading to syndiotactic PEA.

with diazoacetates.<sup>24</sup> PEA might thus be formed via consecutive (migratory)  $\alpha$ -insertions of metal-bound carbenes into the Rh–C bond of the growing chain (Scheme 4).

**(a) Stereocontrol.** Since no ancillary ligand effect on the stereoselectivity was observed, we propose that the insertions into the Rh–CH(COOEt)P fragment (P = polymeryl) are sterically controlled by the configuration of the Rh-bound carbon atom of the growing chain (propagation under “chain-end control”). This is illustrated by the Newman projections in Figure 7. Stereoselective propagation under chain-end control<sup>25</sup> has been observed in a number of insertion polymerizations, including the Pd-mediated alternating copolymerization of CO with styrene.<sup>26</sup>

Migratory carbene insertions involving stereogenic Rh–\*CH(COOEt)P methine carbons (\*C) in configuration *S* experience least steric hindrance when the *re*-face of the rhodium–carbene is attacked. This yields a new Rh–\*CH(COOEt)P methine carbon in configuration *R*, which in turn preferentially attacks the *si*-face of a carbene (Figure 7). We thus expect formation of a syndiotactic polymer, having a regular arrangement of alternating *R* and *S* configurations concerning the stereogenic carbons of the polymer backbone.<sup>27</sup> This seems in agreement with the DSC data, but a definitive assignment of the polymer configuration still requires additional investigations.

(24) Maxwell, J. L.; Brown, K. C.; Bartley, D. W.; Kodadek, T. *Science* **1992**, *256*, 1544–1547.

(25) Bovey, F. A.; Tiers, G. V. D. *J. Polym. Sci.* **1960**, *44*, 173.

(26) (a) Corradini, P.; De Rosa, C.; Panunzi, A.; Petrucci, G.; Pino, P. *Chimia* **1990**, *44* (3), 52–54. (b) Wong, P. K.; Drent, E.; Pino, P.; Corradini, P.; Petrucci, G. Eur. Pat. Appl. 410543, 1991.

## Conclusions

Rh-mediated polymerization of carbenes, generated from ethyl diazoacetate, results in formation of a new highly stereoregular polymer with a high molecular mass: poly(ethyl 2-ylideneacetate) (PEA). Diazoacetates containing other ester functionalities can also be polymerized. The polymers contain polar functional side groups at each carbon of the carbon-chain backbone.

PEA is obtained as a white amorphous solid but can be crystallized to obtain a material with a high degree of crystallinity (~70%). The stereocontrol in the formation of PEA most likely involves propagation under chain-end control. Therefore, stereoregular PEA is likely syndiotactic, which seems in agreement with the relatively high  $T_g$  of the material.

We expect that these new polymers, having a unique structure, will have special material properties. Further studies, in which we focus of the structure and properties of these new materials, are underway.

**Acknowledgment.** This work was supported by The Netherlands Organization for Scientific Research (NWO-CW), the Radboud University of Nijmegen, and the University of Amsterdam. We thank J. Opsteen, R. Bovee, and Dr. A. Kros for their assistance with the SEC/MALLS measurements. We thank P. J. Aarnoutse for her assistance with the MALDI-TOF measurements.

**Supporting Information Available:** Experimental procedures and crystallographic data for **1a**, **2a,b**, and **3**, details on SEC/MALLS, NMR, X-ray diffraction, and DSC/TGA polymer characterization, and MM2 and SCF-MO NMR property calculations. This material is available free of charge via the Internet at <http://pubs.acs.org>.

JA058722J

(27) IUPAC Glossary of Basic Terms in Polymers Science. *Pure Appl. Chem.* **1996**, *68/12*, 2287–2311.